Journal of ELECTRONIC MATERIALS, Vol. 39, No. 9, 2010
DOI: 10.1007/s11664-010-1287-0

Fabrication of Thermoelectric Devices by Applying Microsystems Technology

L.M. GONCALVES,[1,3] P. ALPUIM,[2] and J.H. CORREIA[1]

1.—Department of Industrial Electronics, University of Minho, Azurem, 4800-058 Guimaraes, Portugal. 2.—Department of Physics, University of Minho, Azurem, 4800-058 Guimaraes, Portugal. 3.—e-mail: lgoncalves@dei.uminho.pt

Microsystems technologies were applied in the fabrication of thermoelectric (TE) microconverters. Common techniques used in microelectromechanical systems (MEMS) fabrication, namely wet etching, lift-off (with SU-8 photoresist), reactive ion etching (RIE), and lithography-electroplating-molding, were compared in the fabrication process of TE microsystems based on Bi, Sb, and Te thin-film compounds. Thin films of bismuth and antimony tellurides were deposited by co-evaporation, with figures of merit comparable to those of bulk materials. Test structures were fabricated using lithography and wet etching. The etching recipe was optimized by varying the etchant dilution and composition until higher etch rates and desired material selectivity were attained. Since the etching process is applied after deposition, this process allows prior deposition of TE materials by any deposition method; thus, films with high figure of merit can be fabricated. Moreover, wet etching does not require the use of expensive equipment.

Key words: Bismuth telluride, thermoelectric, microcooler, energy harvesting

INTRODUCTION

In recent years, research on thermoelectrics has extended beyond conventional areas to include fields such as microtechnology and nanofabrication. Nanostructured materials, based on quantum wells[1] or quantum dots,[2] can improve the performance of thermoelectric (TE) materials, increasing the figure of merit,[3] defined as $ZT = \alpha^2\rho^{-1}\lambda^{-1}$ (where α is the Seebeck coefficient, ρ is the electrical resistivity, and λ is the thermal conductivity). A high figure of merit will allow TE cooling to compete with conventional refrigeration. On the other hand, increasing demand for autonomous power sources to supply low-power wireless electronic microdevices brings about the need for standalone, long-lived, renewable, inexpensive power sources, for which TE generators may be the answer. These devices are based on the Seebeck effect, which transforms a small temperature gradient into an electric voltage. A single Bi_2Te_3–Sb_2Te_3 thermocouple junction can generate only 300 μV/K. In order to achieve a voltage usable in microelectronics from a small temperature difference (less than 10°C), 4000 thermocouples must be connected in series. If so many thermocouples are to be fitted into a 1 cm^2 device, each thermocouple must be about 100 μm × 200 μm. Fabrication techniques used to produce macrosized TE devices cannot be used for fabrication of such microdevices. Instead, microsystems technology should be used. TE materials can be made in the form of thin films, using conventional deposition processes (physical and chemical vapor deposition or electrochemical deposition). The small dimensions typical of microdevices can be obtained by photolithography patterning. Although these techniques are commonly used in silicon microelectronics, their application to TE tellurium alloys is still under development. Tellurium alloys (n-type Bi_2Te_3 and p-type Sb_2Te_3 or $Bi_xSb_{2-x}Te_3$) are well-established TE materials for operation near room

(Received July 10, 2009; accepted May 10, 2010; published online June 9, 2010)

temperature and are widely used in the TE industry as part of bulk conventional Peltier modules, since they have a high Seebeck coefficient near room temperature, low electrical resistivity, and relatively low thermal conductivity.

THIN-FILM DEPOSITION

Deposition of Bi, Sb, and Te thin-film compounds can be done by electrochemical deposition (ECD), metalorganic chemical vapor deposition (MOCVD), pulsed laser deposition (PLD), sputtering, and thermal evaporation.[4–11] Independently of the technique used, good control of film composition and crystalline structure is very important to fabricate films with a high figure of merit. Previous work by our group[3] showed that the optimum composition to maximize the figure of merit is obtained at a Te content in the range of 60% to 65%.[12] When directly evaporating either Bi_2Te_3, Sb_2Te_3 or $Bi_xSb_{2-x}Te_3$, the materials decompose and the final composition of the film does not match the initial composition of the evaporant. This is due to the very different vapor pressures of the elemental substances Bi, Sb, and Te. Moreover, when thicker films are deposited, the composition differs from the surface layers into the bulk.[4] This effect is more evident in thermal evaporation than in sputtering, since the temperature necessary to evaporate thermally promotes decomposition of the source materials. To overcome this problem, thermal co-evaporation is normally used[5–7] (co-sputtering is also used for similar reasons[8,9]). In this way, the deposition rate of each element (Bi, Sb, or Te) is controlled independently, and an optimal composition can be achieved. The power factor, defined as $PF = \alpha^2\rho^{-1}$, of films deposited by co-evaporation (calculated using the measured Seebeck coefficient α and electrical resistivity ρ) as a function of composition (measured by energy-dispersive x-ray spectroscopy, EDX) is presented in Fig. 1. It can be seen that the maximum power factor was obtained with substrate heated to 270°C and tellurium content in the range of 60 at.% to 65 at.%.

The importance of the film structure for high figure of merit was demonstrated before.[6,10] The structure of the films presented herein varies from amorphous to polycrystalline. Films with a higher crystalline fraction usually have a lower electrical resistivity. The polycrystalline structure also has the effect of decreasing the film thermal conductivity[10] (compared with a single crystal), which increases the figure of merit. The crystalline structure can be controlled by the substrate temperature during deposition or with postdeposition annealing under controlled atmosphere. However, as mentioned above, due to the different vapor pressures of tellurium, bismuth, and antimony, the composition of the films becomes tellurium poor if the substrate is heated during deposition above 200°C. The influence of substrate temperature on the power factor in films deposited by co-evaporation is presented in Fig. 2. A low deposition rate (below 5 Å/s) normally correlates with a high crystalline fraction, resulting in a higher figure of merit. However, a low deposition rate limits the film thickness that can be deposited. Using co-sputtering or ECD, higher deposition rates can be obtained. Böttner et al.[9] reported a deposition rate of 5 μm/h using co-sputtering, and Jeffrey Snyder et al.[11] from JPL fabricated a device with 20-μm-high TE columns by using ECD. Table I compares the TE properties of Bi_2Te_3 and Sb_2Te_3 or $Bi_xSb_{2-x}Te_3$ films deposited by different techniques. The first two lines in the table refer to the results in this work, and the remaining lines refer to other results from the literature.

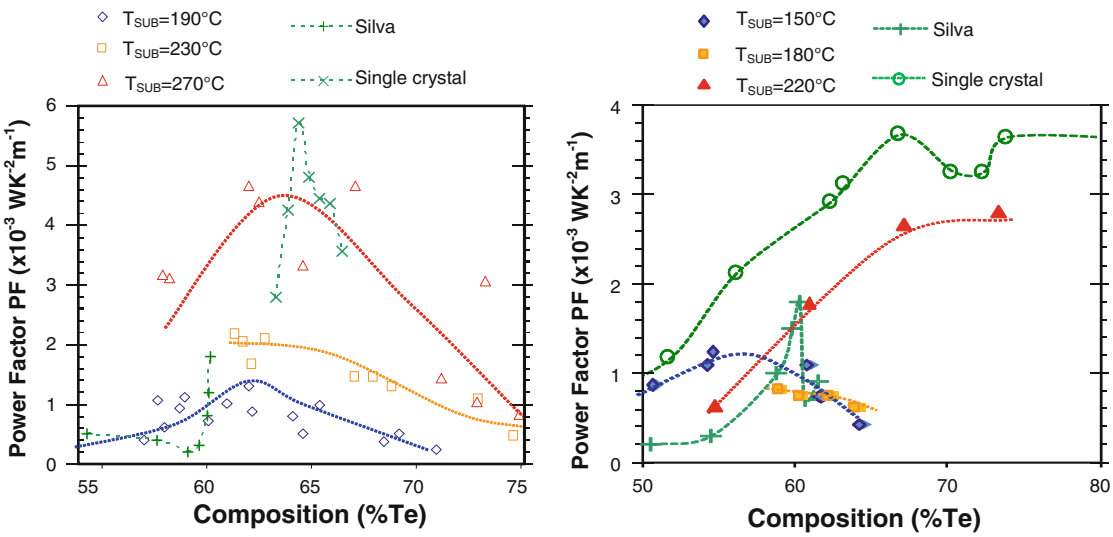

Fig. 1. Power factor of Bi_2Te_3 (*left*) and Sb_2Te_3 (*right*) films deposited by co-evaporation[10] plotted as a function of composition and substrate temperature during deposition (T_{SUB}) (*lines* are guides to the eye). Results obtained in co-evaporated thin films from da Silva et al.[6] and from single crystals[12] are also presented.

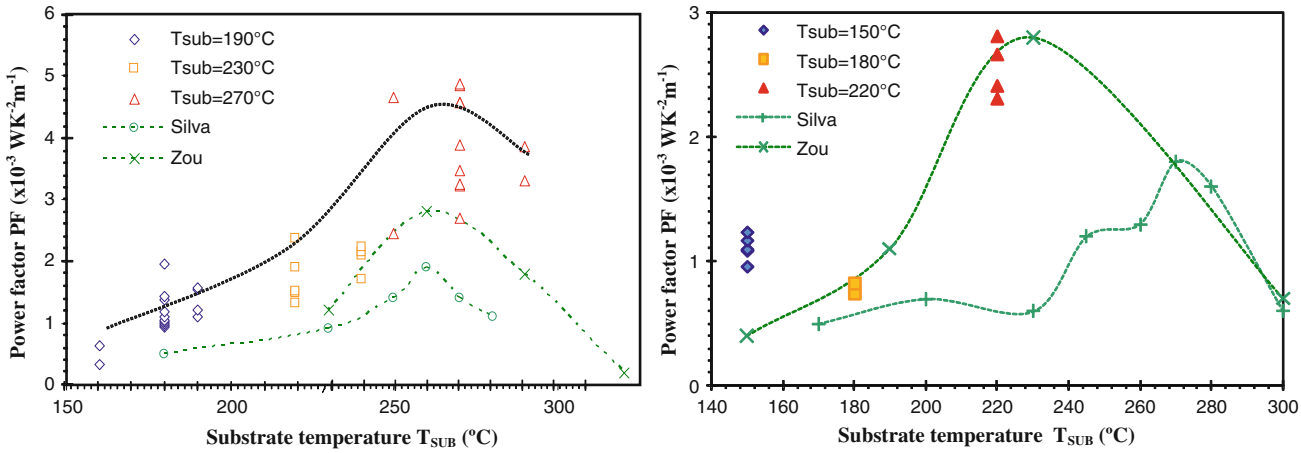

Fig. 2. Power factor of selected Bi_2Te_3 (*left*) and Sb_2Te_3 (*right*) films plotted as a function of substrate temperature T_{SUB} (*lines* are guides to the eye). Results from Zou et al.[5] and da Silva et al.[6] are also presented for comparison.

Table I. Properties of selected Bi_2Te_3 and $Bi_xSb_{2-x}Te_3$ films in this work and from the literature

Material	Type	Deposition Technique	Seebeck, α (μV/K)	Resistivity, ρ ($\mu\Omega$ m)	Power Factor, PF (10^{-3} W/K^2/m)	Figure of Merit, Z (10^{-3}/K)	Reference	Notes
Bi_2Te_3	*n*	Co-evaporation	−220	0.6	4.57	3.03	This work	
Sb_2Te_3	*p*	Co-evaporation	188	12.6	2.81	1.87	This work	
Bi_2Te_3	*n*	Electrochemical	−60	10	0.36	–	Ref. 17	
Bi_2Te_3	*n*	MOCVD	−210	12	3.7	2.48	Ref. 18	(1)
Sb_2Te_3	*p*	MOCVD	−110	3.5	3.46	–	Ref. 18	
Bi_2Te_3	*p*	MOCVD	190	78	0.46	2.5	Ref. 19	(1)
Bi_2Te_3	*n*	MOCVD	−218	6.9	6.9	–	Ref. 20	
$Bi_{0.5}Sb_{1.5}Te_3$	*p*	Flash	230	17	3.1	2.9	Ref. 21	
$Bi_2Te_{2.72}Se_{0.3}$	*n*	Flash	−200	15	2.7	–	Ref. 22	
$Bi_{0.5}Sb_{1.5}Te_3$	*p*	Flash	240	12	4.8	–	Ref. 22	
$Bi_{1.8}Sb_{0.2}Te_{2.7}Se_{0.3}$	*n*	Sputtering	−235	47	1.2	–	Ref. 23	(2)
Bi_2Te_3	*n*	Co-sputtering	−160	16.3	1.6	–	Ref. 9	(3)
$(BiSb)_2Te_3$	*p*	Co-sputtering	175	12.1	2.5	–	Ref. 9	(3)
$Bi_2Se_{0.3}Te_{2.7}$	*n*	Sputtering	−160	20	1.3	–	Ref. 24	
$Bi_{0.5}Sb_{1.5}Te_3$	*p*	Sputtering	210	25	1.8	–	Ref. 24	
Bi_2Te_3	*n*	Co-sputtering	−55	10	0.3	–	Ref. 25	
Bi_2Te_3	*n*	Co-evaporation	−228	13.0	4.0	2.7	Ref. 26	(1)
Sb_2Te_3	*p*	Co-evaporation	171	10.4	2.8	1.76	Ref. 26	(1)
Bi_2Te_3	*n*	Co-evaporation	−228	28.3	1.8	–	Ref. 6	
Sb_2Te_3	*p*	Co-evaporation	149	12.5	1.78	–	Ref. 6	

Notes: (1) Z estimated by the author; (2) Doped with CuBr; (3) Power factor of 3×10^{-3} W/K^2/m and 4×10^{-3} W/K^2/m, respectively, for *n*- and *p*-type were reported later by the same authors,[27] but no reference of other thermoelectric properties was found.

PATTERNING PROCESSES

Common techniques used in microelectromechanical systems (MEMS) fabrication, namely wet etching, lift-off (with SU-8 photoresist), reactive ion etching (RIE), and lithography-electroplating-molding (LIGA), have been successfully tried for the fabrication of TE microstructures.

Böttner et al.[9] used the RIE technique to pattern thick films of Bi, Sb, and Te compounds, using photoresist as an etching mask. Two wafers with patterned TE materials were soldered to create the columnar TE device. Each wafer contained *n*- or *p*-type material, deposited on top of metal contacts and a soldering material that covers the semiconductor layer. The wafers were then aligned and soldered. This process allows one to obtain TE materials with crystalline structure by means of heating the substrate during growth of the TE material.

Researchers at JPL[11] used a process imported from MEMS technology (LIGA) to fabricate microcolumns of TE materials. Au/Cr contacts were

deposited and patterned on the substrate. Thick photoresist was patterned to create holes, where TE materials were deposited by ECD. A Au/Ni layer was deposited and patterned over the structures to create top contacts. Photoresist, Au, and Cr layers were etched, creating the complete device. Using this process, high columns could be formed, but the figure of merit of TE materials deposited by ECD was low.

Lift-off can also be used with TE materials. Photoresist is spun and patterned to define the lift-off pattern, and the TE materials are deposited on top. The photoresist is then removed, removing also the TE material on top of it and creating the structures. The process is repeated for each fabrication step. The technique was applied by da Silva and Kaviany,[13] using SU-8 photoresist and thermally co-evaporated Bi_2Te_3 and Sb_2Te_3 thin films. The yield of this process was low, in particular for small TE elements (7 μm $\times$ 7 μm). Due to the maximum working temperature of photoresist, the substrate cannot be heated above 170°C during deposition of TE materials and the figure of merit is lower than that obtained at higher substrate temperature.

Shafai and Brett[14] has reported on the possibility of using nitric acid (HNO_3) and hydrochloric acid (HCl) diluted in water (H_2O) for etching Bi_2Te_3, but that work was not extended to full characterization of the process, and it was not applied to other tellurium compounds. Recent work from Sedky et al.[15] showed suspended Bi_2Te_3 microstructures fabricated by wet etching. In the present work, wet etching is used for the fabrication of a thin-film planar device. Thin films of Bi_2Te_3 and Sb_2Te_3 (1 μm thick) were deposited on polyimide substrates by thermal co-evaporation. PKP negative photoresist (Transene Company Inc.) was spun onto the surface of the sample, and test structures were patterned by photolithography. Different etching solutions were prepared[16] using water, pure HNO_3, and 37% (by volume) HCl diluted in water, and the effect of etchant composition on the etch rate and on the quality of the patterned structures was recorded. Figure 3 shows the etch rate of Bi_2Te_3 and Sb_2Te_3 films in $(1-x)HNO_3$:(x)HCl solution (diluted 70% in water, by volume). A higher percentage of HCl (%HCl/%$HNO_3 > 0.5$) induces cracking of the film, and peeling occurs. Using only HNO_3 (diluted 70% in water, by volume), Bi_2Te_3 is etched at ~300 nm/s, and the Sb_2Te_3 etch rate is below 6 nm/s. This ratio of 50$\times$ can be useful to selectively pattern devices with both materials, etching Bi_2Te_3 with HNO_3 while leaving Sb_2Te_3 films untouched. However, this method cannot be used when $Bi_xSb_{2-x}Te_3$ replaces Sb_2Te_3. The etching attack in this solution on $Bi_xSb_{2-x}Te_3$ is similar to that suffered by Bi_2Te_3, even for small values of x. Figures 4 and 5 show the influence of etchant dilution (in water) on the etch rate of Bi_2Te_3 and Sb_2Te_3 films, respectively. A composition of the etchant solution in the range of 10:1:20 to 10:6:40 in HNO_3:HCl:H_2O produces the best results. With dilution above 80 vol.% of water, the etch rate is very low and peeling of the film from the substrate occurs. With dilutions below 60%, the etch rate is very high and it becomes difficult to control the etching end point. Table II shows the etch rates of Bi_2Te_3, Sb_2Te_3, Cr, and Al in HNO_3:HCl:H_2O, HNO_3, aluminum etchant ($16H_3PO_4$:$1HNO_3$:1HAc:$2H_2O$, Transene Company

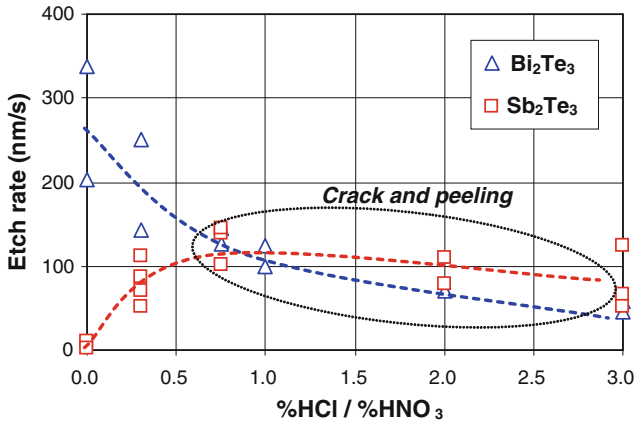

Fig. 3. Etch rate of Bi_2Te_3 and Sb_2Te_3 films in $(1-x)HNO_3$:(x)HCl solution (diluted 70% in water, by volume).

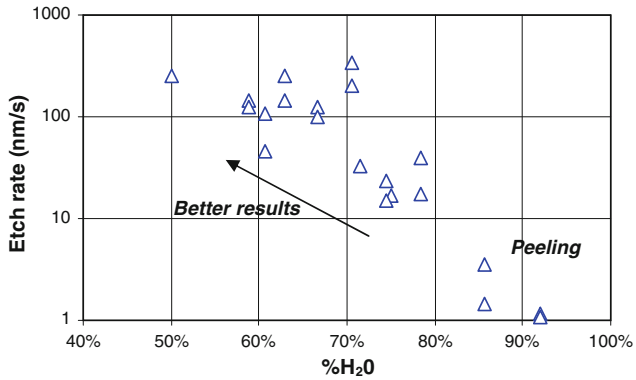

Fig. 4. Influence of dilution of 10:3 HNO_3:HCl solution on the etch rate of Bi_2Te_3 film.

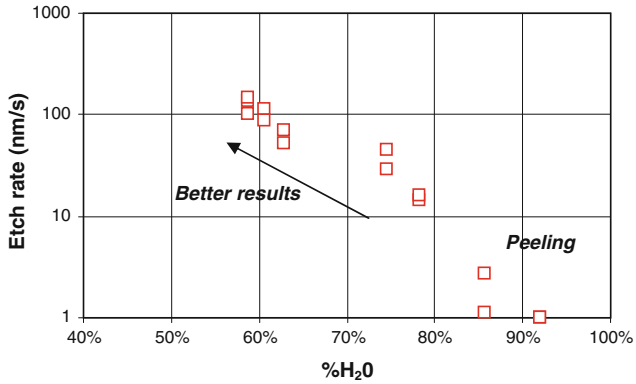

Fig. 5. Influence of dilution of 10:3 HNO_3:HCl solution on the etch rate of Sb_2Te_3 film.

Table II. Summary of etch rates

Material Etchant	Bi_2Te_3 (Å/s)	Sb_2Te_3 (Å/s)	Aluminum (Å/s)	Nickel (Å/s)
Al—Transene type A	8	5	10–80	<0.1
Cr—Transene 1020	~20	<1	–	10–40
$3HNO_3$:1HCl (dil. 70% H_2O)	2000	800	<2	<0.2
HNO_3 (dil. 70% H_2O)	2500	50	<0.1	<0.1

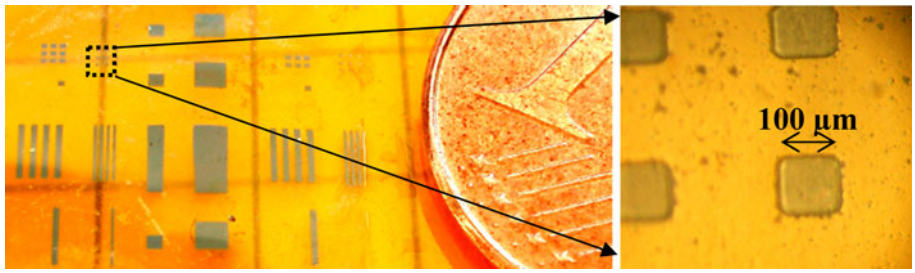

Fig. 6. Top view of test structures of thermoelectric films patterned by wet etching.

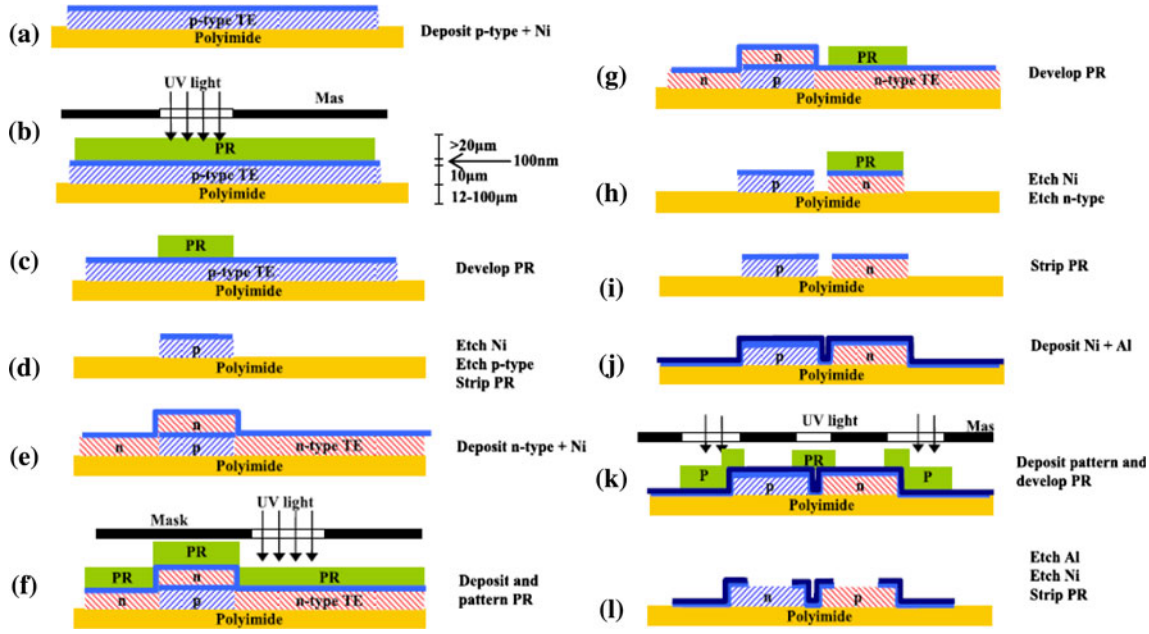

Fig. 7. Fabrication steps of a thermoelectric device.

Inc. type A, where Ac represents acetic acid), and chromium etchant (based on ceric ammonium nitrate, Transene Company Inc., type 1020). The selectivity between different etchants for different materials allows the choice of different possible etchant combinations in order to fabricate a complete device. Figure 6 shows the patterned structures used for etchant evaluation studies.

Figure 7 shows the fabrication process steps for TE converters. The *p*-type Sb_2Te_3 film is deposited by thermal co-evaporation followed by a thin layer (100 nm) of nickel (Fig. 7a). The use of a thin Ni layer avoids diffusion of the TE material into the next deposited layers. The photoresist is spun, and *p*-type elements are patterned by photolithography (Fig. 7b, c). Nickel is etched in a chromium etchant (Transene 1020), and the TE film is patterned by wet etching in a HNO_3:HCl bath. In Fig. 7d, the photoresist is removed. The *n*-type film is then deposited by co-evaporation, followed by deposition of a 100 nm nickel layer (Fig. 7e). The photoresist is applied and patterned by photolithography for *n*-type element definition (Fig. 7f, g). Nickel is etched in a chromium etchant (Transene 1020), the *n*-type film is etched in HNO_3 (Fig. 7h), and photoresist is removed (Fig. 7i). Contacts are deposited, starting

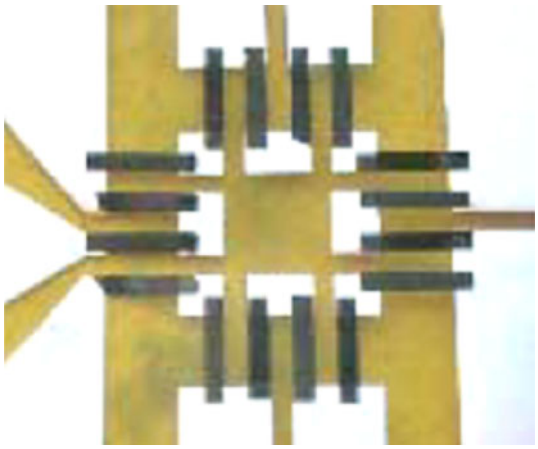

Fig. 8. Thermoelectric device fabricated on a polyimide flexible substrate using thin-film deposition and patterned by wet etching.

with a 100-nm layer of Ni, followed by 1 μm of Al (Fig. 7j). The photoresist is spun, and contacts are patterned by photolithography (Fig. 7k). Ni is etched in a chromium etchant (Transene 1020), and Al with a standard aluminum etchant (Transene type A). The photoresist is removed (Fig. 7l). A protective layer of Si_3N_4 can also be deposited at low temperature by hot-wire chemical vapor deposition (HW-CVD) and patterned if required, depending on the application. Figure 8 shows a planar TE device composed of eight pairs of Bi_2Te_3/Sb_2Te_3 and their metal contacts, fabricated on a flexible polyimide substrate, using the process just described. The performance of this device was presented and discussed elsewhere.[16] A temperature difference of 5°C was measured between the hot and cold sides of the device when a current of 6 mA was applied between contacts.

CONCLUSIONS

Several techniques were compared for the deposition of Bi, Sb, and Te thin-film compounds. The influence of substrate temperature on film structure and composition and the effect of these film properties on the figure of merit of TE junctions are reported. The best films were obtained with the substrate heated to 200°C to 270°C and with a tellurium content in the range of 60 at.% to 65 at.%.

Semiconductor TE films were patterned by wet etching in a HNO_3:HCl:H_2O solution. The influence of etchant composition on the etch rate and pattern quality was studied and reported. The best results were obtained with an etch rate of ~200 nm/s in 10:3:30 HNO_3:HCl:H_2O. This solution etches aluminum and chromium films with an etch rate below 0.2 nm/s, allowing selectivity higher than 1000 to TE materials. Bi_2Te_3 can also be etched in 30% HNO_3 etchant, with selectivity higher than 50 to Sb_2Te_3 films.

ACKNOWLEDGEMENT

This work was supported by FCT/PTDC/EEA-ENE/66855/2006.

REFERENCES

1. R. Venkatasubramanian, E. Siivola, T. Colpitts, and B. O'Quinn, *Nature* 413, 597 (2001).
2. D.M. Rowe, eds., *CRC Handbook of Thermoelectrics—Macro to Nano* (London: CRC, 2005).
3. M.S. Dresselhaus, G. Chen, M.Y. Tang, R.G. Yang, H. Lee, D.Z. Wang, Z.F. Ren, J.-P. Fleurial, and P. Gogna, *Adv. Mater.* 19, 1 (2007).
4. L.W. Silva and M. Kaviany, *ASME Proc. of IMECE'02*, New Orleans, USA, Nov (2002), pp. 17–22.
5. H. Zou, D.M. Rowe, and S.G.K. Williams, *Thin Solid Films* 408, 270 (2002).
6. L.W. da Silva, M. Kaviany, and C. Uher, *J. Appl. Phys.* 97, 114903 (2005).
7. L.M. Goncalves, J.G. Rocha, C. Couto, P. Alpuim, G. Min, D.M. Rowe, and J.H. Correia, *J. Microelectromech. Syst.* 17, S168 (2007).
8. D.-h. Kim, E. Byon, G.-H. Lee, and S. Cho, *Thin Solid Films* 510, 148 (2005).
9. H. Böttner, J. Nurnus, A. Gavrikov, G. Kuhner, M. Jagle, C. Kunzel, D. Eberhard, G. Plescher, A. Schubert, and K.H. Schlereth, *J. Microelectromech. Syst.* 13, 414 (2004).
10. L.M. Goncalves, C. Couto, P. Alpuim, A.G. Rolo, F. Völklein, and J.H. Correia, *Thin Solid Films* 518, 2816 (2010).
11. G. Jeffrey Snyder, J.R. Lim, C.-k. Huang, and J.-P. Fleurial, *Nat. Mater.* 2, 528 (2003).
12. H. Scherrer and S. Scherrer, *CRC Handbook of Thermoelectrics*, ed. D.M. Rowe (1987), pp. 211–237.
13. L.W. da Silva and M. Kaviany, *J. Microelectromech. Syst.* 14, 1110 (2005).
14. C. Shafai and M.J. Brett, *J. Vacuum Sci. Technol. A* 17-1, 305 (2001).
15. S. Sedky, A. Kamal, M. Yomn, H. Bakr, R. Ghannam, V. Leonov, and P. Fiorini, *Proc. International Conference Transducers 09*, Denver, CO, USA (2009).
16. L.M. Goncalves, C. Couto, P. Alpuim, and J.H. Correia, *J. Microelectromech. Syst.* 18, 064008 (2008).
17. J.R. Lim, G.J. Snyder, C.-K. Huang, J.A. Herman, M.A. Ryanand, and I.-P. Fleurial, *Proc. International Conference on Thermoelectrics* (2002).
18. A. Giani, A. Boulouz, F. Pascal-Delannoy, A. Foucaran, E. Charles, and A. Boyer, *Mater. Sci. Eng. B* 64, 19 (1999).
19. A. Giani, F. Pascal-Delannoy, A. Foucaran, and A. Boyer, *Thin Solid Films* 303, 1 (1997).
20. A. Boulouz, A. Giani, F. Pascal-Delannoy, M. Boulouz, A. Foucaran, and A. Boyer, *J. Cryst. Growth* 194, 336 (1998).
21. F. Völklein, V. Baier, U. Dillner, and E. Kessler, *Thin Solid Films* 187, 253 (1990).
22. A. Foucaran, A. Sackda, A. Giani, F. Pascal-Delannoy, and A. Boyer, *Mater. Sci. Eng. B* 52, 154 (1998).
23. E. Kessler, A. Ihring, V. Baier, A. Franke, and U. Dillner, *Proceedings of 11th International Conference Sensor 2003*, Vol. II, Nürnberg (2003), pp. 249–254.
24. M. Stordeur and I. Stark, *IEEE Proc. 16th Int. Conf. on Thermoelectrics*, Dresden, Germany (1997), p. 575.
25. D. Kim, E. Byon, G. Lee, and S. Cho, *Thin Solid Films* 510, 148 (2006).
26. H. Zou, D.M. Rowe, and G. Min, *J. Cryst. Growth* 222, 82 (2001).
27. H. Bottner, J. Nurnus, A. Schubert, and F. Volkert, *Proc. International Conference on Thermoelectrics ICT'07*, Korea (2007).